



Trans. Nonferrous Met. Soc. China 24(2014) 310-315

Transactions of Nonferrous Metals Society of China

www.tnmsc.cn

Microstructure of Mg-8Zn-4Al-1Ca aged alloy

Yun DONG, Xiao-ping LIN, Jie YE, Run-guo ZHENG, Na HE School of Materials and Metallurgy, Northeast University, Shenyang 110819, China Received 20 January 2013; accepted 8 May 2013

Abstract: The microstructure of Mg-8Zn-4Al-1Ca aged alloy was investigated by TEM and HRTEM. The results show that the hardening produced in the Mg-8Zn-4Al-1Ca alloy is considerably higher than that in the Mg-8Zn-4Al alloy. A dense dispersion of disc-like Ca₂Mg₆Zn₃ precipitates are formed in Mg-8Zn-4Al-1Ca alloy aged at 160 °C for 16 h. In addition, the lattice distortions, honeycomb-looking Moiré fringes, edge dislocations and dislocation loop also exist in the microstructure. The precipitates of alloy aged at 160 °C for 48 h are coarse disc-like and fine dispersed grainy. When the alloy is subjected to aging at 160 °C for 227 h, the microstructure consists of numerous MgZn₂ precipitates and Ca₂Mg₆Zn₃ precipitates. All the analyses show that Ca is a particularly effective trace addition in improving the age-hardening and postponing the formation of MgZn₂ precipitates in Mg-8Zn-4Al alloy aged at 160 °C.

Key words: Mg-8Zn-4Al-1Ca alloy; age hardening; Ca₂Mg₆Zn₃; Moiré fringe

1 Introduction

Mg-Zn-based alloys remarkable have age-hardening response, when typically subjected to artificial aging at temperatures above about 150 °C. The precipitation in the alloys generally takes place through the formation of many intermediate phases: SSSS-> GP zone/ β'_1 (rods or blocky precipitates $\perp [0001]_{Mg}$, possibly MgZn₂ or Mg₄Zn₇) $\rightarrow \beta'_2$ (laths \perp [0001]_{Mg} or coarse plates $//[0001]_{Mg}$, MgZn₂) $\rightarrow \beta$ equilibrium phase (MgZn or Mg₂Zn₃) [1-8]. The $(1\overline{1}00)$ habit plane of MgZn' precipitate can prevent dislocation from slipping on the basal plane of magnesium, therefore, the MgZn' precipitate has been considered to be the most effective strengthening phase. However, the solubility of Zn (8.1%, mass fraction) in the magnesium is lower than that of Al (12.7%), so the MgZn' precipitate has a low density. Moreover, due to the thermal instability of MgZn' precipitate, the MgZn' precipitate is easy to transform into the coarse lath precipitate, which significantly affects the strength of the alloy. Therefore, it has become a research emphasis to restrain the transformation. BETTLES et al [9] studied the age-hardening behaviour in Mg-4% Zn micro-alloyed with Ca. The results indicated that the addition of trace amounts of Ca to a

Mg-4%Zn alloy has led to a significant enhancement of the age-hardening response by the refinement of the resulting precipitate microstructure. NIE and MUDDLE [10] reported an improvement in peak hardness of Mg-1Ca-1Zn alloy over Mg-1Ca binary alloy by the formation of ternary precipitates. LEVI et al [11] and GENG et al [12] have studied the effect of Ca additions on age-hardening and microstructure of Mg-Zn-based alloys. They indicated that Ca could provide significant precipitation hardening. In addition, Al also could significantly improve the age hardening response of Mg-Zn alloy. OH-ISHI et al [13] indicated that the addition of Al to Mg-Zn alloys could cause more variation of the morphology and finer distribution of precipitates. LIN et al [14] also indicated that the addition of appropriate amount of Al to Mg-Zn-based alloy can increase the density of the strengthening phase and improve the aging hardness of the alloy. JAYARAJ [15] studied the enhanced precipitation hardening of Mg-Ca alloy by Al addition. The results indicated that the addition of Al to Mg-Ca alloy causes more ordered monolayer GP zones and increases the age hardening.

In this work, the effect of 1% Ca (mass fraction) addition on age-hardening and microstructure of Mg-8Zn-4Al alloy was studied.

DOI: 10.1016/S1003-6326(14)63062-4

2 Experimental

An alloy having a composition of Mg-8Zn-4Al-1Ca (mass fraction) was prepared from magnesium (99.8%), aluminum (99.9%), zinc (99.9%) and calcium (99.9%) with an electrical resistance furnace under protective gas of 0.1% SF₆+99.9% CO₂. The melts were heated to 720 °C, held for 20 min and then poured into a 15 mm (diameter)×200 mm pre-heated permanent mould made of steel. The alloy was solution heat treated at 380 °C for 10 h prior to quenching in cold water and aging. Artificial aging was performed at 160 °C in an oil bath. The age hardening responses were measured with a Vickers hardness tester (HXD-1000) under a load of 4.9 N (500 g) and the values reported here were averaged from at least 10 measurements. Transmission electron microscopy (TEM) observation was performed using Philips CM200 at 200 kV. High resolution TEM (HRTEM) observation was performed using JEOL JEM-2010FEF at 300 kV. Scanning electron microscopy (SEM) observation was performed using Hitachi S-4800. The phase composition was characterized by X-ray diffraction (XRD).

3 Results and discussion

3.1 Age hardening

Figure 1 shows the age-hardening curves of Mg-8Zn-4A1-1Ca alloy and the Mg-8Zn-4A1 alloy aged at 160 °C. The hardening produced in the Mg-8Zn-4A1-1Ca alloy is considerably higher than that in the Mg-8Zn-4A1 alloy. For the Mg-8Zn-4A1 alloy, the peak hardness is HV78.53 and it is achieved after 48 h of aging. Then the hardness value decreases rapidly for the duration of the experiment. However, for the Mg-8Zn-4A1-1Ca alloy, the kinetics of aging at initial stage is considerably accelerated and reaches

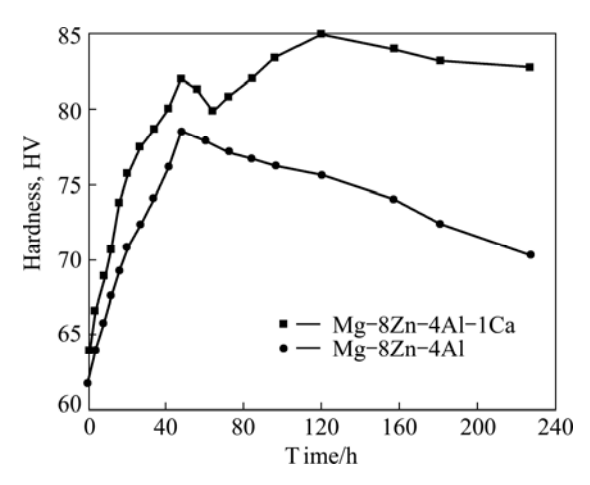


Fig. 1 Hardening curves of Mg-8Zn-4A1-1Ca alloy and Mg-8Zn-4A1 alloy aged at 160 °C

96.51% of its maximal hardness after 48 h. Then, the hardness value decreases significantly and increases after 72 h of aging. The hardness reaches the peak (HV 85.03) after 120 h of aging. As aging time prolongs, the hardness value gradually decreases as a result of over aging, but the descending rate of hardness value is extremely slow. The curves indicate that although the amount of Ca dissolved in the Mg-8Zn-4A1 alloy is only 1%, it has a markedly beneficial effect on the precipitation process during aging.

3.2 Microstructure

3.2.1 Microstructure of Mg-8Zn-4A1-1Ca alloy aged at 160 °C for 16 h

Figure 2(a) shows the microstructure of Mg-8Zn-4Al-1Ca alloy aged at 160 °C for 16 h. The image was taken with the electron beam parallel to the [0001]_{Mg}. A dense dispersion of circular-shaped precipitates with 10-40 nm in diameter is seen in the microstructure. Figure 2(b) shows the HRTEM image of the circular-shaped precipitate. The inset in Fig. 2(b) is the fast Fourier transforms (FFT) corresponding to the circular-shaped precipitate. The FFT pattern could be indexed consistently according to a hexagonal structure, with lattice parameters a=0.9725 nm, c=1.014 nm. This structure of the circular-shaped precipitate was similar to that of theCa₂Mg₆Zn₃. Figure 2(c) shows the HRTEM image of the microstructure of matrix. Some dispersively distributed fine precipitates (indicated by black arrows) with 3-5nm diameter, possibly also circular-shaped precipitates, are observed in microstructure. The variation in phase caused by these precipitates is clearly visible. The distinguishable contrast may be caused by the segregation of Ca or Zn atoms.

Figure 3(a) also shows the HRTEM image of the microstructure of Mg-8Zn-4Al-1Ca alloy aged at 160 °C for 16 h. The fast Fourier transform (FFT) (inset in Fig. 3(a)) of the magnesiummatrix could be indexed according to the [2111] zone axis. Some edge dislocations and dislocation loop are shown in the Fourier-filtered image (inset in Fig. 3(a)) of the region A. The lattice distortion in the core of the edge dislocations is visible. SAITO et al [16] studied the microstructural changes of GP zones in an Mg-1.5%Gd-1%Zn (mole fraction) alloy with HAADF-STEM technique. Their results indicated that there is a fairly variable nature in microstructures of the GP zones with an advance of aging, demonstrating that the aging behaviour associated with the GP zones is as follows: wavy GP zone→planar GP zone→band shaped (multi-layer) GP zones→ stacking faults. It is well known that solute atoms are easy to aggregate at the crystal defects. So, the

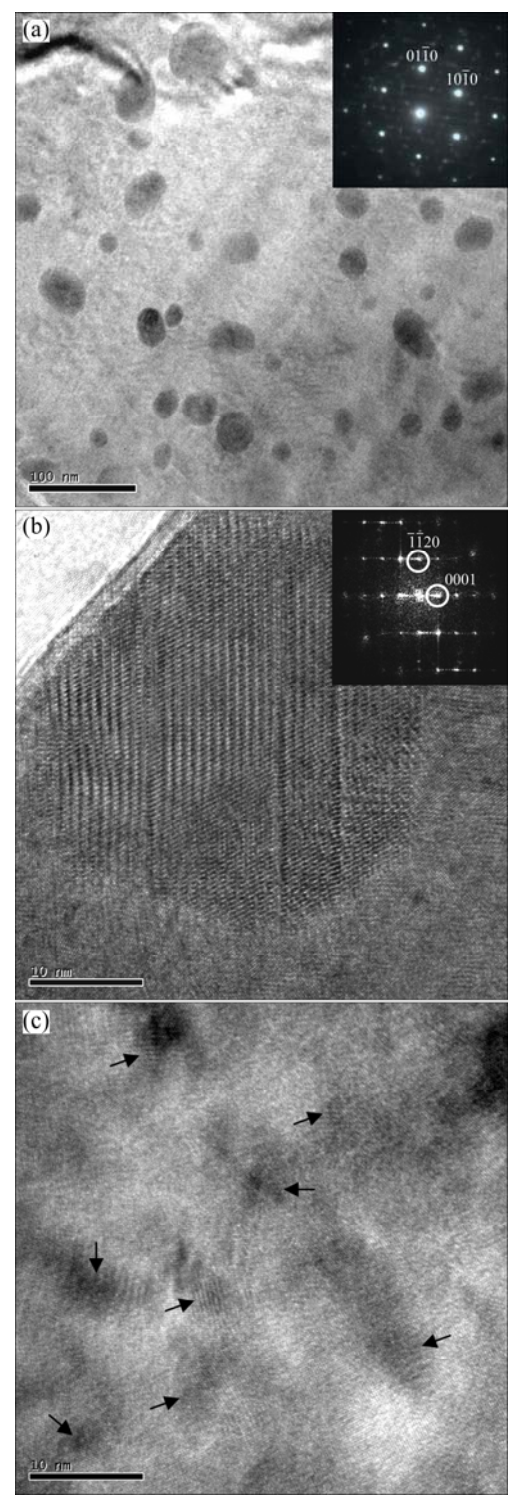


Fig. 2 $[0001]_{Mg}$ TEM image of microstructure of Mg-8Zn-4Al-1Ca alloy aged at 160 °C for 16 h (a), HRTEM image of circular-shaped precipitate (b) and HRTEM image of microstructure of matrix (c)

dislocations are conducive to the aggregation of the solute atoms, thus increasing the nucleation rate of precipitates. In addition, the honeycomb-looking Moiré fringes (circled by white circle) are also shown in the microstructure. Figure 3(b) shows the FFT corresponding

to the honeycomb-looking moiré fringes. It shows that besides the diffraction spots from Mg Matrix, the FFT pattern also includes some diffraction spots produced by the Ca₂Mg₆Zn₃ precipitates. So, the honeycomb-looking Moiré fringes are possibly produced by the overlap of three hexagonal lattices, as shown in Fig. 3(b). The strong spot (indicated by white arrow) is also produced by the overlap of three spots. Figure 3(c) also shows the HRTEM image of the microstructure of Mg-8Zn-4Al-1Ca alloy aged at 160 °C for 16 h. The corresponding FFT is inset in Fig. 3(c). The elongated precipitate (indicated by white arrow) with the thickness of 2–3 nm is shown in the microstructure. The atomic arrangement at the interface of the elongated precipitate and the magnesiummatrix can been clearly seen in Fig. 3(d). The interface between the elongated precipitate and magnesiummatrix is a coherent interface with a strong lattice distortion. Along [0001]_{Mg}, the interplanar spacing of the elongated precipitation (d') is about double that of the magnesium matrix (d). It is well known that the magnesium is a hexagonal with lattice parameters a=0.3209 nm, c=0.5211nm, while the lattice parameters of $Ca_2Mg_6Zn_3$ are a=0.9725 nm, c=1.014 nm. The c-axis of the Ca₂Mg₆Zn₃ also is about double that of the Mg, combining with the analysis of Fig. 2. It is presumed that the elongated precipitate is possibly Ca₂Mg₆Zn₃ phase. The Ca₂Mg₆Zn₃ is a circular-shaped precipitate on $\{0001\}_{Mg}$ in Fig. 2(a) and a elongated precipitate on $\{2\overline{1}\overline{1}0\}_{Mg}$ in Fig. 3(c). So it is reasonable to believe that the Ca₂Mg₆Zn₃ precipitate has a morphology of disc-like. Furthermore, it is noteworthy that the the Ca₂Mg₆Zn₃precipitate retains a coherent relationship with α -Mg matrix, and mismatch between the two crystals along c-axis is δ =2.544%, so the coherence strengthening is stimulated.

The analysis for Figs. 2 and 3 shows that a dense dispersion of disc-like Ca₂Mg₆Zn₃ precipitates is formed in Mg-8Zn-4Al-1Ca alloy aged at 160 °C for 16 h. In addition, the lattice distortions, honeycomb-looking Moiré fringes, edge dislocations and dislocation loop also exist in the microstructure.

3.2.2 Microstructure of Mg-8Zn-4A1-1Ca alloy aged at 160 °C for 48 h

Figure 4 shows the microstructure of Mg-8Zn-4Al-1Ca alloy aged at 160 °C for 48 h. A dense dispersion of disc-like precipitates is shown in Fig. 4(a). These precipitates are dispersively distributed in the grain or along the grain boundary. Figure 4(b) shows that the disc-like precipitates formed in the grain have a tendency to grow large with the extension of aging time; however, a number of fine dispersed grainy precipitates also exist in the microstructure. The fine dispersed grainy precipitates are very beneficial to improving the age-hardening of Mg-8Zn-4Al-1Ca alloy. No rod-like

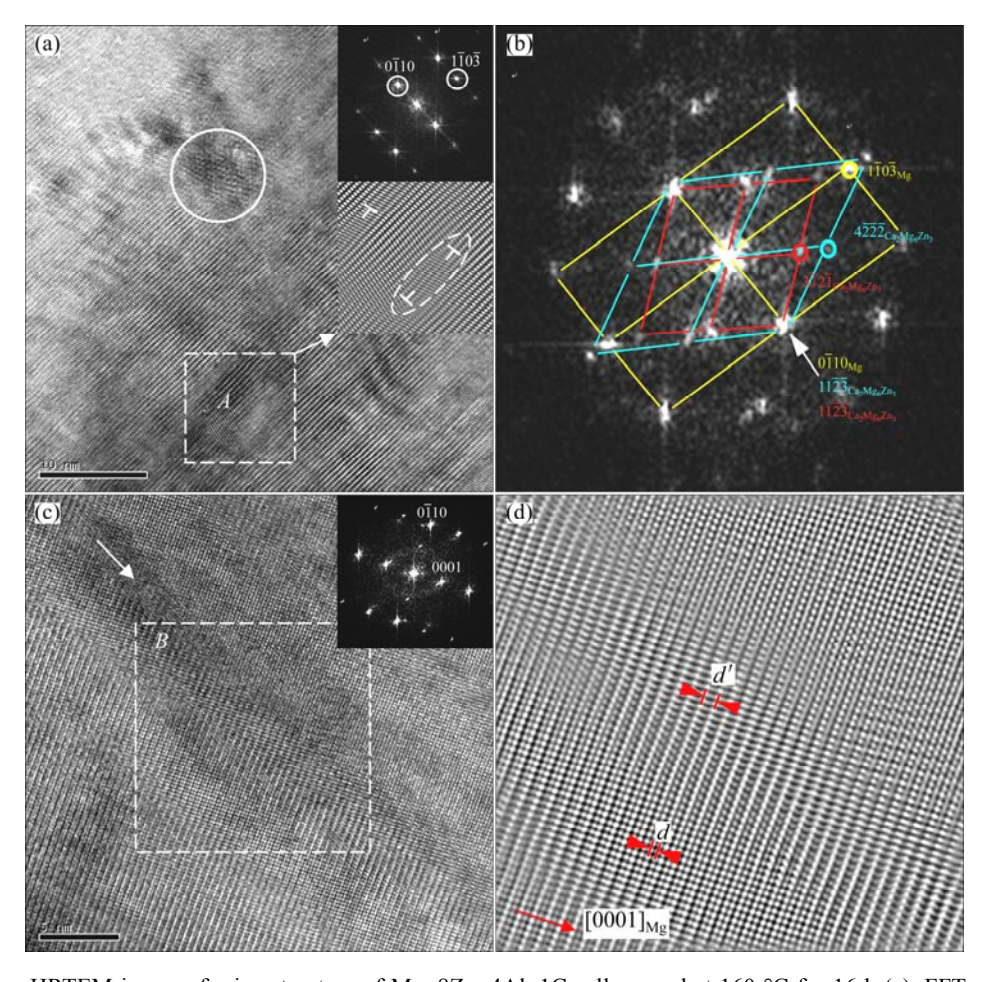


Fig. 3 $[2\overline{1}\overline{1}1]_{Mg}$ HRTEM image of microstructure of Mg-8Zn-4Al-1Ca alloy aged at 160 °C for 16 h (a), FFT corresponding to honeycomb-looking moiré fringes in Fig. 3(a) (b), $[2\overline{1}\overline{1}0]_{Mg}$ HRTEM image of microstructure of Mg-8Zn-4Al-1Ca alloy aged at 160 °C for 16 h (c) and Fourier-filtered image of region *B* in Fig. 3(c) (d)

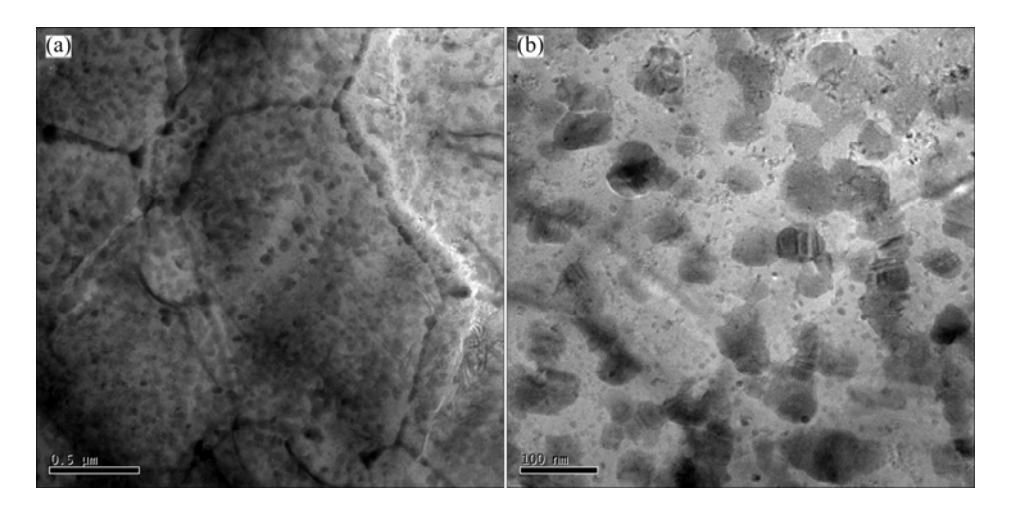


Fig. 4 TEM image of microstructures of Mg-8Zn-4Al-1Ca alloy aged at 160 °C for 48 h: (a) Low magnification; (b) High magnification

or coarse lath $MgZn_2$ precipitates are found in the microstructure.

3.2.3 Microstructure of Mg-8Zn-4A1-1Ca alloy aged at $160~^{\circ}\text{C}$ for 227 h

Figure 5 shows the SEM images of the

microstructure of Mg-8Zn-4Al-1Ca alloy aged at 160 °C for 227 h. A dense dispersion of elongated precipitates viewed edge-on along with the same direction is shown in Fig. 5(a). The morphology of the elongated precipitates is shown more clearly in the inset

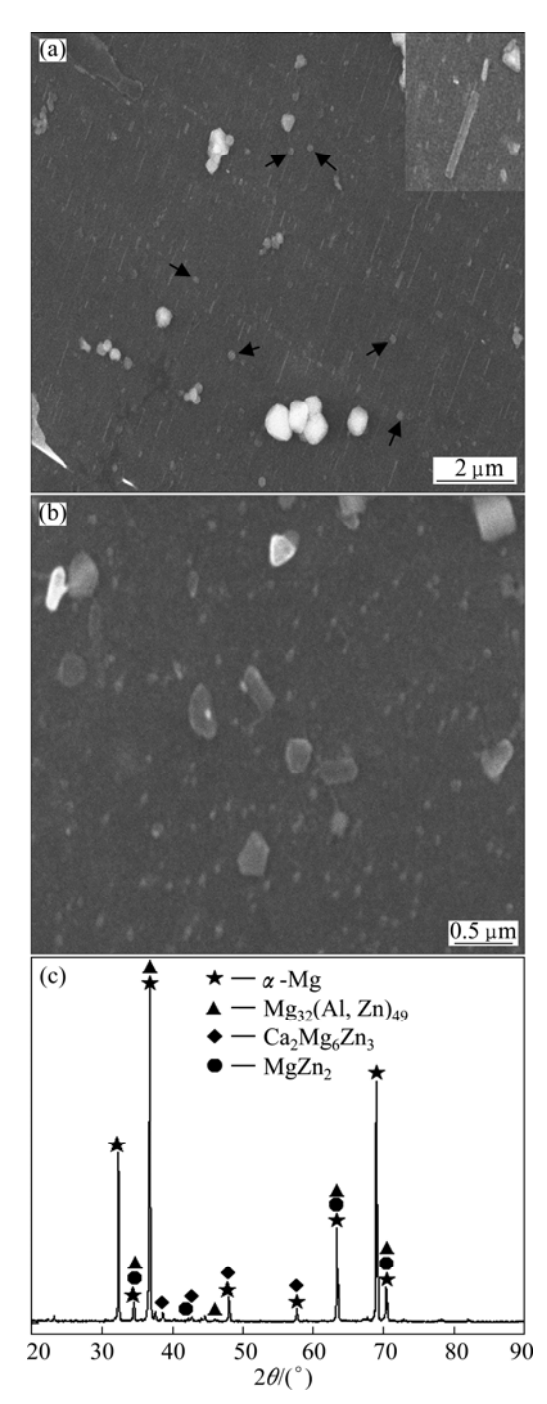


Fig. 5 Low magnification SEM image (a), high magnification SEM image (b) and XRD pattern (c) of Mg-8Zn-4Al-1Ca alloy aged at 160 °C for 227 h

of Fig. 5(a). In addition to the elongated precipitates, a less fraction of circular-shaped precipitates (indicated by black arrows) is also observed in the microstructure. When the microstructure in Fig. 5(a) is further amplified, a large number of fine dispersed grainy precipitates, as shown in Fig. 5(b). Similar microstructure is observed in the Mg-8Zn-4Al-1Ca alloy aged at 160 °C for 48 h. According to this, it is presumed that these fine dispersed grainy precipitates existing in Fig. 5(b) may be the same as that in Fig. 4(b). The X-ray diffraction (XRD) pattern

taken from the alloy is shown in Fig. 5(c), in which peaks can be indexed as arising from three phases, α -Mg (matrix), Mg₃₂(Al,Zn)₄₉, Ca₂Mg₆Zn₃ and MgZn₂. On the basis of the microanalysis and XRD pattern, these elongated precipitates are identified as MgZn₂ and these circular-shaped precipitates are identified as Ca₂Mg₆Zn₃.

For the Mg–8Zn–4Al–1Ca aged alloy, all the analyses show that no rod-like or coarse lath MgZn₂precipitates are formed at initial stage and peak-aged state; however, there are a large number of elongated MgZn₂ precipitates at the over-aging stage. Meanwhile, the age-hardening of the alloy is very high at the over-aging stage. So, it is reasonable to believe that Ca is a particularly effective trace addition in improving the age-hardening and postponing the formation of MgZn₂ precipitates in Mg–8Zn–4Al alloy aged at 160 °C.

4 Conclusions

- 1) The hardening produced in the Mg-8Zn-4A1-1Ca alloy is considerably higher than that in the Mg-8Zn-4A1 alloy. For the Mg-8Zn-4A1-1Ca alloy, the kinetics of aging at initial stage is considerably accelerated, and reaches 96.51% of its maximal hardness after 48 h. The hardness reaches the peak after 120 h of aging. As aging time prolongs, the descending rate of hardness value is extremely slow.
- 2) A dense dispersion of disc-like Ca₂Mg₆Zn₃ precipitates are formed in Mg-8Zn-4Al-1Ca alloy aged at 160 °C for 16 h. In addition, the lattice distortions, honeycomb-looking Moiré fringes, edge dislocations and dislocation loop also exist in the microstructure.
- 3) The precipitates of alloy aged at 160 °C for 48 h are coarse disc-like precipitates and fine dispersed grainy precipitates. The fine dispersed grainy precipitates can increase the age-hardening of Mg–8Zn–4Al–1Ca alloy. When the alloy is subjected to aging for 227 h at 160 °C, the microstructure consists of numerous MgZn₂ precipitates and $Ca_2Mg_6Zn_3$ precipitates.

References

- [1] DING Wen-jiang. Science and technology of magnesium alloy [M]. Beijing: Science Press, 2007: 1–20. (in Chinese)
- [2] BUHA J. Reduced temperature (22–100 °C) ageing of an Mg–Zn alloy [J]. Materials Science and Engineering A, 2008, 492(1): 11–19.
- [3] GAO X, NIE J F. Characterization of strengthening precipitate phases in a Mg-Zn alloy [J]. Scripta Materialia, 2007, 56(8): 645-648.
- [4] BUHA J. The effect of Ba on the microstructure and age hardening of an Mg–Zn alloy [J]. Materials Science and Engineering A, 2008, 491(1): 70–79.
- [5] BUHA J. The effect of micro-alloying addition of Cr on age hardening of an Mg–Zn alloy [J]. Materials Science and Engineering A, 2008, 492(1): 293–299.

- [6] BUHA J. Characterisation of precipitates in an aged Mg–Zn–Ti alloy[J]. Journal of Alloys and Compounds, 2009, 472(1): 171–177.
- [7] BUHA J. Mechanical properties of naturally aged Mg–Zn–Cu–Mn alloy [J]. Materials Science and Engineering A, 2008, 489(1): 127–137.
- [8] BUHA J. Grain refinement and improved age hardening of Mg-Zn alloy by a trace amount of V [J]. Acta Materialia, 2008, 56(14): 3533-3542.
- [9] BETTLES C J, GIBSON M A, VENKATESAN K. Enhanced age-hardening behaviour in Mg-4 wt.% Zn micro-alloyed with Ca [J]. Scripta Materialia, 2004, 51(3): 193–197.
- [10] NIE J F, MUDDLE B C. Precipitation hardening of Mg-Ca(-Zn) alloys [J]. Scripta Materialia, 1997, 37(10): 1475–1481.
- [11] LEVI G, AVRAHAM S, ZILBEROV A, BAMBERGER M. Solidification, solution treatment and age hardening of a Mg– 1.6wt.%Ca-3.2wt.%Zn alloy [J]. Acta Materialia, 2006, 54(2): 523-530.

- [12] GENG L, ZHANG B P, LI A B, DONG C C. Microstructure and mechanical properties of Mg-4.0 Zn-0.5 Ca alloy [J]. Materials Letters, 2009, 63(5): 557-559.
- [13] OH-ISHI K, HONO K, SHIN K S. Effect of pre-aging and Al addition on age-hardening and microstructure in Mg-6wt% Zn alloys [J]. Materials Science and Engineering A, 2008, 496(1): 425–433.
- [14] LIN X P, DONG Y, YE J, SONG B Y. The microstructure of Mg-4Zn-2Al-0.5 Ca aged alloy [J]. Materials Science and Engineering A, 2012, 538: 231-235.
- [15] JAYARAJ J, MENDIS C L, OHKUBO T, OH-ISHI K, HONO K. Enhanced precipitation hardening of Mg-Ca alloy by Al addition [J]. Scripta Materialia, 2010, 63(8): 831-834.
- [16] SAITO K, YASUHARA A, HIRAGA K. Microstructural changes of Guinier–Preston zones in an Mg–1.5 at% Gd–1at% Zn alloy studied by HAADF-STEM technique [J]. Journal of Alloys and Compounds, 2011, 509(5): 2031–2038.

Mg-8Zn-4Al-1Ca 合金的时效微观组织

董 允, 林小娉, 叶 杰, 郑润国, 何 娜

东北大学 材料与冶金学院, 沈阳 110819

摘 要:利用 TEM 和 HRTEM 研究 Mg-8Zn-4Al-1Ca 合金的时效微观组织。结果表明:Mg-8Zn-4Al-1Ca 合金较 Mg-8Zn-4Al 合金时效硬度显著增高。Mg-8Zn-4Al-1Ca 合金在 160 °C 时效 16 h,有大量的盘状 $Ca_2Mg_6Zn_3$ 相沉淀弥散析出,此外,合金的微观组织中还存在晶格畸变、蜂窝状的莫尔条纹、刃型位错及位错环;经 48 h 时效后合金中沉淀相为粗大的盘状沉淀相和细小、弥散的粒状沉淀相;经 227 h 时时效后后,其组织中存在大量 $MgZn_2$ 相和 $Ca_2Mg_6Zn_3$ 相。因此,在 Mg-8Zn-4Al-1Ca 时效 160 °C 的合金中添加 Ca 元素能有效提高合金的时效 硬度及促进 $MgZn_2$ 强化相的生成。

关键词: Mg-8Zn-4Al-1Ca 合金; 时效强化; Ca₂Mg₆Zn₃; 莫尔条纹

(Edited by Chao WANG)